Appl. Phys. A 69, 225–232 (1999) / Digital Object Identifier (DOI) 10.1007/s003399900072

Applied Physics A
Materials
Science & Processing

Defect passivation using ultrasound treatment: fundamentals and application

S. Ostapenko

Center for Microelectronics Research, University of South Florida, 4202 E Fowler Avenue, Tampa, Florida 33620, USA
(Fax: +1-813/9743-610, E-mail: ostapenk@eng.usf.edu)

Received: 1 March 1999/Accepted: 28 March 1999/Published online: 14 June 1999

Abstract. Ultrasonic vibrations introduced into semiconductor thin-films can trigger defect reactions, which are beneficial for electronic materials and devices. This type of semiconductor processing is assigned as *ultrasound treatment (UST)*. The UST technology was initially developed in compound semiconductors and recently successfully applied to Si-based materials. The analysis of UST effects is performed within a general scenario of three-step point-defect gettering comprised of the (a) release, (b) diffusion, and (c) capture of the defects. As a demonstrating vehicle of UST mechanisms, the experimental data on ultrasonically enhanced diffusion of atomic hydrogen in thin polycrystalline Si films are discussed. UST applied to plasma-hydrogenated films improves the homogeneity of recombination and transport properties. Ultrasound promotes a passivation of grain boundary defects as revealed using scanning photoluminescence spectroscopy, contact potential difference with nano-scale resolution, and sheet resistance measurements. The results favor a model of trap-limited hydrogen diffusion facilitated by ultrasound. Illustrative examples of the UST application for electronic devices are presented.

PACS: 71.55.-i; 73.50.-h; 78.55.Ap

Discovered in the late 60s and extensively explored since the 80s [1], the ultrasound stimulated processes in Ge, Si, and compound semiconductors attracted the attention of various research groups. It has been demonstrated that ultrasonic vibrations generated into a crystal can stimulate numerous defect reactions and, as a consequence, benefit the design of electronic materials with improved and even superior characteristics. This new technological approach is recognized as a potentially powerful tool for defect engineering to improve performance and reliability of electronic devices [2].

Ultrasonic processing of semiconductors and relevant mechanisms are referred to as *ultrasound treatment* (hereafter the UST). The UST effect can be assigned as a stable improvement of material properties and device parameters after they have been affected by ultrasound. The UST method utilizes a fundamental concept in solids. It is based on a coupling of the ultrasonic vibrations with the extended crystal defects such as dislocations, grain boundaries, and precipitates, which interact with point defects, both of impurity and native origin, such as vacancies and self-interstitials. Being absorbed at extended defects, ultrasonic vibrations trigger defect reactions as will be illustrated in the following sections. Therefore, UST realizes a method of defect engineering in semiconductors that benefits material quality. The UST method is based on a solid and well-understood physical concept. In real crystals, defects and their complexes can exist in a stable, unstable, or metastable configuration. The bottom-line of the UST technology is that mechanical vibrations can assist a system of crystal defects in reaching a favorable position, which has the lowest total energy; therefore, this is the preferable, stable state. On the other hand, UST is a simple and intuitive approach. Many people are experienced with a simple 'ultrasound treatment' in their daily routine without noticing it. The following illustrative case reveals the utility of mechanical vibrations to solve a simple problem.

Look at gas bubbles in a liquid. Imagine you decided to have a drink of soda and, before drinking, you are trying to get rid of the gas bubbles, which are strongly attached to the glass walls. Knock on the glass with your finger and immediately some of the trapped bubbles will be released and run to the surface. What happened? Acoustic vibrations were generated in the glass and transferred their energy to the bubbles. This extra energy was enough to release the trapped bubbles by breaking their molecular bonds of surface tension with the glass. This simple example is surprisingly similar to what the ultrasound is doing to enhance defect passivation with hydrogen in poly-Si films, a material for a new generation of active-matrix liquid-crystal displays and thin-film solar cells. It will be shown in Sect. 3, that trapped atomic hydrogen can be released by UST and moved to more stable positions at dangling bonds, which benefit transport properties of electrons and holes.

This article describes the UST method and apparatus, and also summarizes UST-controlled defect reactions, rele-

vant mechanisms, and application issues. Particular examples of the enhanced hydrogenation in thin poly-Si films provide a deeper insight into a specific UST mechanism.

1 UST method and apparatus

Ultrasonic vibrations have to be delivered to a semiconductor material or electronic device to perform UST processing. Three different techniques to generate ultrasonic vibrations are applicable.

1.1 External piezoelectric transducer

The most general method utilizes an external source for the ultrasound, such as a resonance piezoelectric transducer. This UST technique has advantages of being a non-contact process in an active device region at the front surface of a wafer. The method is applicable for large-scale materials and devices, such as 8" Si-wafers and 12" or for greater flat-panel displays [3]. This UST approach is also compatible with conventional device-processing steps: deposition, annealing, doping, and passivation. A schematic of the UST unit – the key element of a large-scale UST station – is shown in Fig. 1. Low-amplitude ultrasonic vibrations are introduced into the UST object: a semiconductor wafer, a thin film on a substrate, or a microelectronics device using a piezoelectric transducer operating in a resonance vibration mode and coupled with the UST object. Typically, a circular transducer is driven by a generator and power amplifier adjusted to the first resonance of its radial or thickness vibrations. The resonance frequency varies from 20 kHz to 100 kHz for radial vibration mode and can be extended into the MHz range using thickness vibrations. This frequency depends on the transducer geometry, vibration mode, material of the piezoelectric transducer, and varies with temperature and UST amplitude. Adjusted to a resonance frequency, the UST transducer generates maximum ultrasonic amplitude, which is quantified by a value of the acoustic strain. The amplitude of acoustic strain is the ratio of the vibrating amplitude to a characteristic size of the transducer (for example, the diameter). In the UST technique, the acoustic strain typically does not exceed 10^{-4} corresponding to the acoustic power of a few W/cm^2. To provide an effective UST processing, the acoustic strain is controlled with a calibrated sensor of acoustic vibrations (non-contact UST probe). The UST temperature can be stabilized from room temperature to the Curie point of the transducer (350 °C for commercial PZT-5A piezoelectric ceramics). A sample has to be placed on a UST chuck composed of one or more UST transducers and tightly pressed against a chemically polished transducer surface using a vacuum contact. A computer system controls the process "in situ" and adjusts the UST parameters: amplitude, frequency, and temperature operating in a feedback loop with the non-contact UST probe and non-contact infrared temperature sensor. This approach has been realized in a multi-transducer UST station, which is capable of processing large-scale wafers by delivery of a quasi-homogeneous distribution of UST amplitudes and temperature from a set of UST transducers to the 12" diagonal samples. The station can be scaled up simply by adding ultrasound transducers at a custom-designed configuration of the UST chuck.

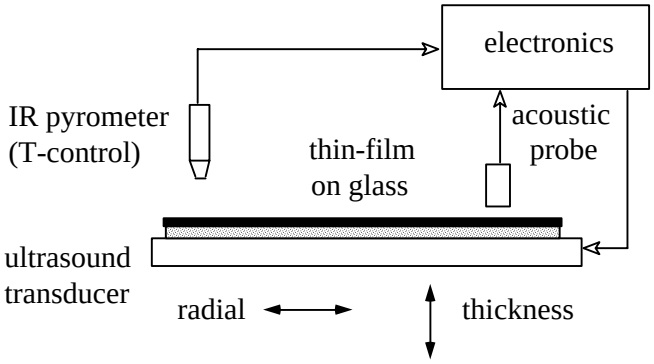

Fig. 1. Schematic of the UST unit for processing of thin-film electronic materials and devices

1.2 Internal piezoelectric effect

UST vibrations can be alternatively generated in materials using the internal piezoelectric effect of a semiconductor. In this case, an ac voltage can be applied via electrodes oriented along specific crystallographic directions (for example along the *c* axis in hexagonal-type crystals) [4]. The ac electric field generates intensive ultrasonic vibrations when its frequency (between 100 kHz and 20 MHz) is adjusted to the acoustic resonance of a sample. This method is limited to semiconductors with a high resistance and possessing a noticeable piezoelectric constant (CdS, CdSe, $CdZnP_2$, and others). It also requires a special sample shaping in the form of an acoustic resonator.

1.3 Pulsed laser excitation

Another UST approach is based on pulsed-laser excitation [5]. The absorption in a crystal of a nanosecond laser pulse (for example a ruby laser with a power density of the order 10^{12} W/cm^2) generates a set of ultrasonic pulses. These ultrasonic pulses propagate across the crystal and, after absorption at crystal defects, perform an efficient UST processing. In this technique, the laser power density has to be carefully controlled to prevent the degradation of a material due to creation of new crystal defects.

2 UST mechanisms (overview)

Although UST effects in semiconductors are well documented experimentally, there are a limited number of conclusive results where partial understanding of relevant physical mechanisms was achieved. Table 1 contain a summary of UST mechanisms suggested in various semiconductor materials. In the following section, a specific topic of UST hydrogenation in poly-Si thin films will be discussed in detail.

UST mechanisms are tightly related to processes of point-defect gettering. Defect gettering was introduced into semiconductors using a terminology from the cathode-ray

Table 1. Ultrasound-stimulated processes in semiconductors

Physical mechanism	Material	Reference
Dissolving of defect clusters and pairs	Cz-Si	[6]
	poly-Si	[7, 8]
	CdHgTe	[9]
	CdS	[10]
	GaAs	[11]
Enhanced diffusion	Ge	[12]
	Si	[13]
	CdS	[5]
Capture of point defects	CdS	[14]
	CdTe	[15]
	ZnCdTe	[16]

tubes (TV screens) where the gettering technique was successfully applied to improve long-term vacuum characteristics of a tube with gas absorbers. In Cz-Si microelectronics, a similar but essentially more sophisticated approach provided for the development of Si-wafers with contamination levels as low as $10^9\,\mathrm{cm}^{-3}$. To achieve this high level of material purity various defect engineering tools were developed, particularly gettering and passivation. According to a general gettering/passivation strategy, the process is comprised of three consecutive steps. The first step is releasing of a bound contamination impurity (Fe, Cu, Cr) or passivating atoms (hydrogen) introduced during wafer/device processing. In the second step, the released atoms diffuse toward the gettering sites (sinks) or passivation targets. Finally, the third step is a capture of contamination impurity at crystallographic defects or binding them with chemical elements at the gettering sites. The ability to control and facilitate any of the gettering/passivation steps can benefit the process efficiency. It was found that UST can positively affect each of the three described steps: release, diffusion and capture of defects as shown in the Table 1.

The understanding of UST mechanisms is largely empirical. In spite of the large number and variety of reported UST effects, only a few of them are supported by theoretical models. One example of such a model includes the quantum theory of point-defect diffusion stimulated by ultrasonic vibrations [17]. In this model, ultrasound reduces the activation energy necessary for diffusion by decreasing the barrier for the diffusing atom. The UST modulation of the phonon distribution and UST-stimulated population of excited states of the diffusing defects are responsible for a decrease of the activation energy. This model is relevant to the data of UST processing shown in Table 1.

The interaction of ultrasound with extended lattice defects – grain boundaries, dislocations, and interfaces – is a key to UST effects. It is generally recognized that ultrasound vibrations are strongly absorbed by these extended defects, which serve at the same time, as gettering sites for doping impurities and contaminations. According to this concept, extended defects can efficiently couple and transfer ultrasound vibrations to point defects.

Polycrystalline-Si thin films are characterized by a high density of grain boundaries, dislocations, and interfaces. They also contain point defects such as doping atoms, contaminants, and their complexes. Therefore, this material is an excellent candidate for UST defect engineering as illustrated in the next section.

3 Hydrogenation enhancement in poly-Si thin films

Polycrystalline-silicon (poly-Si) thin films on glass or fused silica substrates are promising for thin-film transistor (TFT) technology in active-matrix liquid-crystal displays as well as for a new generation of solar cells for terrestrial application. Compared with similar devices using hydrogenated amorphous-silicon films, poly-Si TFTs have improved operational parameters due to substantially higher electron mobility. However, grain boundary states and interface defects in poly-Si lead to a high off-state current and affect the threshold voltage. A conventional approach to passivate these defect states and to reduce inter-grain barriers for electron transport is to apply plasma hydrogenation. The hydrogen defect passivation occurs in two steps: plasma penetration and a subsequent atomic hydrogen diffusion. Unfortunately, the diffusion of hydrogen in poly-Si is slow compared with single-crystal silicon due to a trap-limiting mechanism at grain boundaries, resulting in a long hydrogenation time (typically 1 h at 300 °C) and electrical inhomogeneity within passivated regions of poly-Si. The trap-limited hydrogen diffusivity in poly-Si films is described by the activation energy of 1.3 to 1.5 eV with a diffusion coefficient given by

$$D_\mathrm{H} = D_\mathrm{Ho}(N_\mathrm{i}/N_\mathrm{t}) = D_\mathrm{o}\exp(-E_\mathrm{o}/kT)\exp(-\Delta E/kT), \quad (1)$$

where D_Ho is the hydrogen diffusivity in crystalline Si with an activation energy of $E_\mathrm{o} = 0.48$ eV; $N_\mathrm{i}/N_\mathrm{t}$ is the ratio of interstitial to trapped hydrogen; and ΔE is the binding energy of trapped atomic hydrogen of the order of $\Delta E \approx 1$ eV. The long annealing time motivates a search for non-traditional approaches in order to improve hydrogenation in poly-Si films. It appears that the atomic hydrogen in poly-Si thin films is a specifically suitable object for UST [7]. Based on experiments, a mechanism of UST-enhanced liberation of the atomic hydrogen from trapping states has been proposed [8]. This UST effect is a "trigger" for fast hydrogen diffusion in poly-Si and ultimately provides an effective passivation of defects at grain boundaries.

3.1 Low-temperature UST

For UST experiments at temperatures below 100 °C, ultrasonic vibrations were generated into 0.35-μm poly-Si films and thin-film transistors through a glass substrate using a circular 50-mm or 75-mm-diameter piezoelectric transducer, as shown in Fig. 1. The UST transducer operated at 25 kHz and 48 kHz of the radial resonance vibrations at temperatures limited by the Curie point of piezoelectric ceramics. This part of the UST study is assigned as low-temperature UST processing, which has important implications for poly-Si thin-film transistors on plastic substrates. The UST effect was monitored by measurements of sheet resistance at room temperature using the four-point-probe method. Concurrently, spatially resolved photoluminescence (PL) and nano-scale contact potential difference mapping using atomic force microscopy were performed.

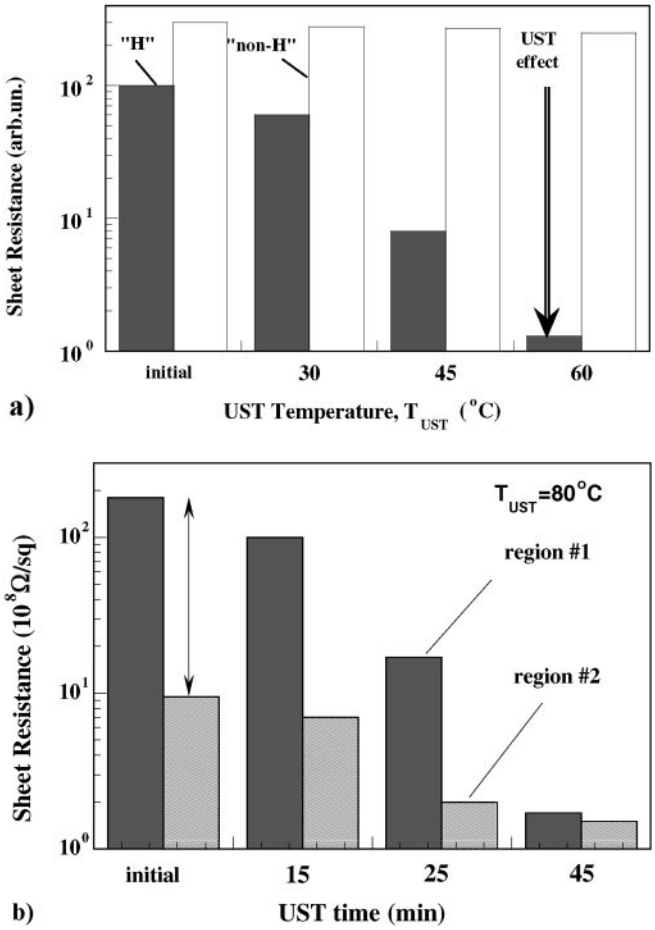

Fig. 2a,b. UST reduces resistance (**a**), and improves homogeneity (**b**) in undoped hydrogenated poly-Si thin films on glass

It was found that conventional plasma hydrogenation applied to undoped poly-Si films reduces the sheet resistance by as much as one order of magnitude due to hydrogenation of grain-boundary dangling bonds. The decreased resistance saturated at a minimum value on the order of 10^9 Ω/sq after 3 to 5 h radio-frequency plasma processing of 0.35-μm films. In the films where plasma hydrogenation process was not completed, the additional strong reduction of resistance after UST by a factor of *two orders of* magnitude was observed (Fig. 2). Importantly, the resistance in non-hydrogenated films was practically unchanged after the same UST. Another feature of the UST effect is an improvement of resistance homogeneity (Fig. 2). By monitoring UST changes of resistance in two different regions of the same film with a high starting electrical inhomogeneity, it was found that the initial difference of more than one order of magnitude in resistance was reduced to approximately 10% after a few consecutive steps of UST. Based on these findings, it is postulated that ultrasound vibrations applied to hydrogenated poly-Si thin films promote a redistribution of the atomic hydrogen in the film. This statement is justified by the following spatially resolved photoluminescence study and the nano-scale contact potential difference mapping.

Photoluminescence (PL) spectroscopy allows for defect monitoring in polycrystalline Si films, and is particularly sensitive to hydrogenation [18]. At 4.2 K, the PL band corresponding to band-tail recombination dominates the luminescence spectrum of films deposited at 625 °C (Fig. 3). With increasing temperature, the band-tail emission is strongly quenched and the broad "defect" PL maximum at about 0.65 eV is retained and persists even at room temperature. The "defect" PL intensity can be used to assess the result of hydrogenation and UST processing on the film recombination properties. We found that "defect"-band PL intensity is increased by a factor of 8 after an electron cyclotron resonance (ECR) plasma hydrogenation (Fig. 4). This is attributed to the passivation of non-radiative centers by atomic hydrogen: dangling silicon bonds at the grain boundaries, which are competing for the capture of minority carriers injected by the excitation laser beam. Spatially resolved room-temperature PL mapping technique with a resolution of 100 μm was used to monitor UST changes in distribution of recombination centers. The result is presented in Fig. 5 in a form of two PL

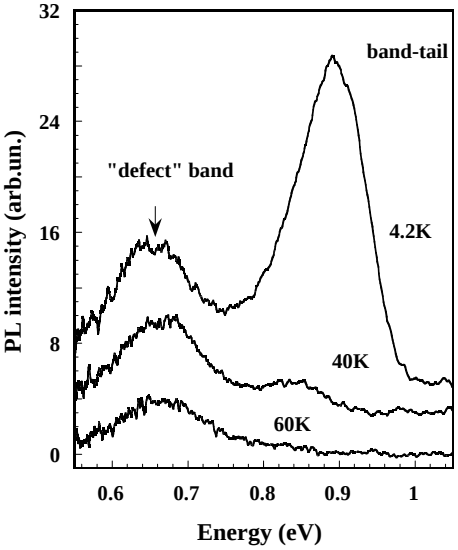

Fig. 3. Photoluminescence spectra of poly-Si thin films on glass deposited at 625 °C measured at different temperatures. Intensity of the 0.65-eV band can be used to monitor quality upgrading of a thin film after hydrogenation and UST

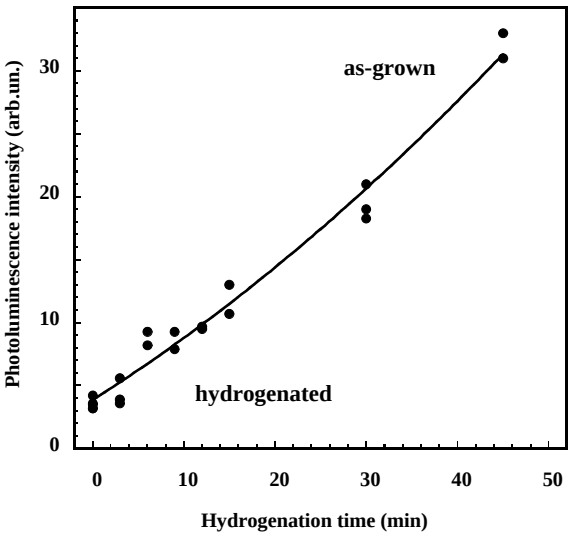

Fig. 4. Increasing of the "defect" band PL intensity after ECR hydrogenation due to passivation of non-radiative centers

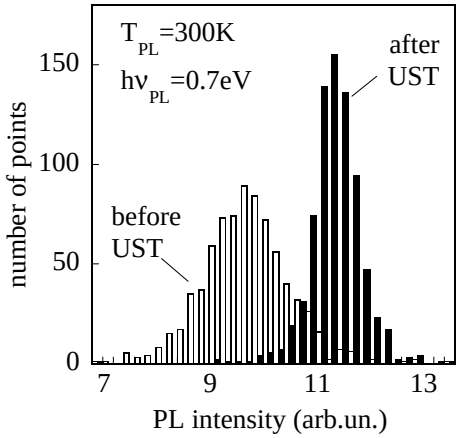

Fig. 5. Two histograms of the "defect" PL band in hydrogenated poly-Si film before and after UST. The treatment (measured at temperature $T_{PL} = 300$ K) increases PL intensity due to redistribution of the atomic hydrogen at grain-boundary defects

histograms of exactly the same hydrogenated film area prior to and after UST. The average value of PL intensity after UST exhibits an additional 30% increase and a narrowing of the histogram half-width by a factor of two. This result is in excellent agreement with the UST-induced improvement of resistance homogeneity measured by the four-point probe.

Another approach to monitor hydrogen passivation is nano-scale contact potential difference (CPD) mapping. The CPD mapping with the spatial resolution of 20 nm was performed in a two-step procedure using the atomic force microscope "Nanoscope III" [7]. In the first step, a regular topographic map of a poly-Si surface was obtained by a standard AFM scan in the "tapping" mode. In the second step, the AFM tip was lifted over the sample surface to the elevation of 20 nm. This constant elevation was accurately maintained by a computer control system during the second map, and therefore, the tip-to-sample capacitance was maintained constant. When an external ac voltage is applied to the AFM tip, the amplitude of the first harmonic of tip oscillations is proportional to the tip-to-sample potential difference. Using a compensating dc voltage, we obtained the spatial distribution of the contact potential difference in the poly-Si surface in a form of CPD map. Details of the CPD technique were published elsewhere [19]. This CPD approach is used in the following ultrasonic treatment experiments.

Figure 6 presents two CPD mappings of a poly-Si thin film subjected to 30 min of ECR plasma hydrogenation (a) and after following UST processing (b). The measurement conditions of CPD mapping specifically the elevation of the tip above the sample surface were precisely maintained. It was noticed that the CPD contrast is gradually reduced with UST time. As a result, the contrast of the CPD map was even more reduced compared to as-grown material after UST processing for 30 min at 70 °C. The UST effect on CPD contrast is quantified by a narrowing of the CPD histogram as shown in Figs. 6c,d.

The important issue of any UST processing is a stability of the UST effect. We found that UST-induced reduction of sheet resistance as depicted in Fig. 2 partially recovers after storage of the films in the dark at room temperature for 12 h [7]. However, the value of resistance after the relaxation was not exactly the same as the initial one, but usually lower. Using consecutive cycles of UST and relaxation, we were able to stabilize the reduced sheet resistance on the level about one order of magnitude lower compared with the initial value. The final value of resistance did not show any significant change for one month at room temperature. This relaxation study suggests that two parallel UST processes occur in hydrogenated films. One of them produces a stable reduction of sheet resistance, while the second promotes a metastable phenomenon. We suggest that the change of CPD contrast depicted in Fig. 6 corresponds to the stable UST effect. Based on presented experimental findings, it can be suggested that these two processes are attributed to (a) stable passivation with atomic hydrogen of grain boundary defects (for example dangling bonds), which is responsible for a permanent change of sheet resistance and CPD contrast, and (b) UST generation of metastable hydrogen-related defects responsible for the relaxation behavior.

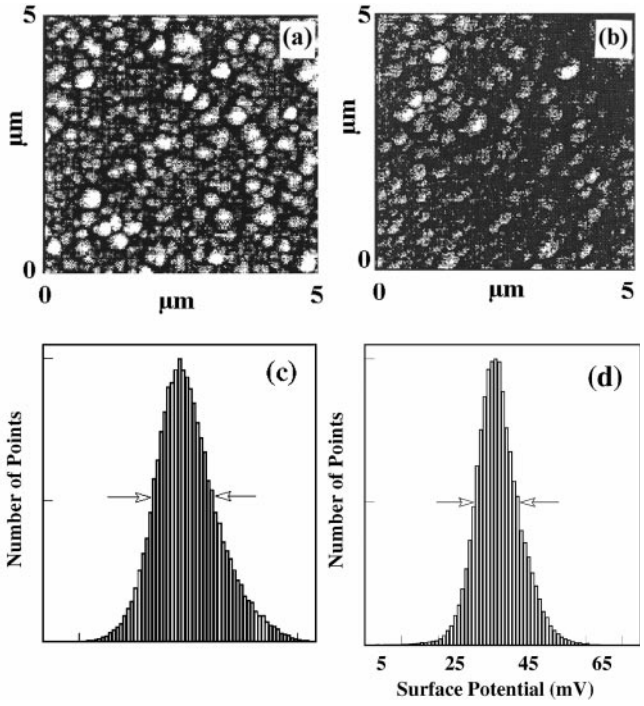

Fig. 6a–d. Contact potential difference mapping in 5 μm × 5 μm area of hydrogenated poly-Si films before UST (**a**) and after UST (**b**). Corresponding histograms of CPD contrast are presented in **c** and **d**. UST parameters are 30 min, 80 °C, and 50 kHz

3.2 High-temperature UST

It was anticipated that the UST is a thermally activated process that can be facilitated above 100 °C. To verify this, poly-Si films thermally recrystallized at 550 °C and annealed at the same temperature as long as 75 h were subjected to UST at temperatures up to 280 °C [8]. This material contains a mixture of amorphous (a-Si) and polycrystalline-Si phases. The volume ratio of crystalline to amorphous phase was quantitatively measured by Raman spectroscopy. The "defect" band shown in Fig. 3 dominates the PL spectrum of poly-Si thin films at 77 K. (There is a shift of the "defect" band from 0.65 to 0.7 eV in some samples). By increasing the annealing time

of 550 °C films up to 75 h, it was found that the intensity of the defect PL band was monotonously increased by a factor of ten tracking the increase of polycrystalline fraction. Therefore, the intensity of the 0.65-eV band can be used to monitor changes of recombination properties in the poly-Si phase of films.

After UST was applied to 550 °C annealed films at T_{UST} = 150–280 °C, two noticeable changes in PL spectrum were observed (see Fig. 7). The first is the increase of the "defect" band intensity by a factor of 2 to 4 (in different samples), which is consistent with data of low-temperature UST processing of hydrogenated poly-Si films shown in Fig. 5. The second and dominant effect is a strong UST activation of a "new" broad PL band with a maximum at 0.98 eV and the half-width of 260 meV at 77 K (referred hereupon as 0.9-eV band). This PL band is clearly distinguished from the band-tail luminescence in polycrystalline silicon (see Fig. 3), having a different line-shape and temperature quenching. We noticed a dramatic enhancement of the 0.9-eV band exceeding *two orders* of magnitude compared to the untreated sample, which requires only a few minutes of UST processing at 250–280 °C. After the UST activation of luminescence is completed the PL spectrum is entirely dominated by the 0.9-eV band. Contrary to low-temperature UST processing, the high-temperature UST effects are stable and did not show any noticeable relaxation.

UST processing was performed at different temperatures between 150 °C and 280 °C. Corresponding points of isothermal kinetics of the 0.9-eV band at two temperatures and their single-exponential fits are shown in Fig. 8. For a comparison, the picture also comprises PL kinetics of a control sample annealed without UST at 280 °C, which proves that the effect of the 0.9-eV band activation is entirely UST related. From the Arrhenius plot of the UST time constant we found the UST activation energy of $E_{UST} = 0.33 \pm 0.05$ eV. The UST kinetic is characterized by a time constant of 3 min at 280 °C. This rate of UST processing is compatible with the best results of plasma hydrogenation of commercial TFTs.

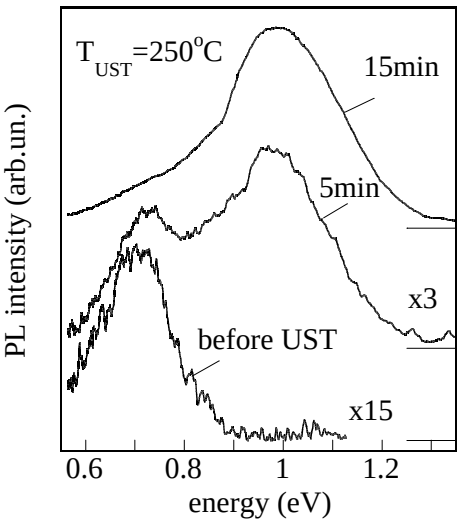

Fig. 7. UST applied at temperatures from 150 °C to 280 °C strongly activates photoluminescence intensity in polycrystalline and amorphous phase of LPCVD thin films deposited at 550 °C and annealed at 550 °C for 24 h

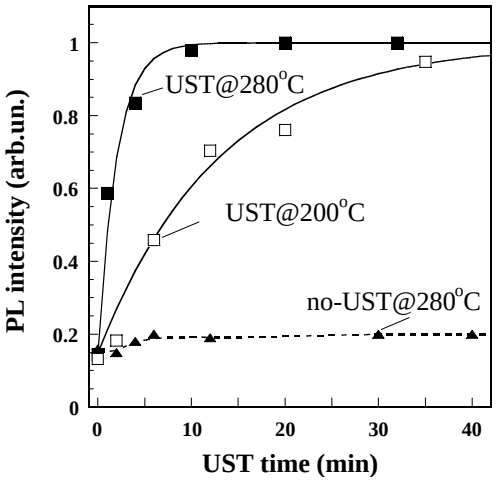

Fig. 8. Isothermal kinetics of the 0.9-eV PL band activated using UST (*points*) and exponential fit (*curves*). Notice that simple annealing at 280 °C without UST does not affect PL intensity

We have strong arguments that the UST-activated 0.9-eV band is related to a residual amorphous phase of of the recrystallized Si films. The saturated intensity of the 0.9-eV band after completion of UST processing is a function of the annealing time at 550 °C and, therefore, depends on the fraction of the α-Si phase in the films as proved by Raman spectroscopy. It was also found that the 0.9-eV band has a maximum intensity in films with a significant fraction of α-Si phase, and is gradually decreased in films where the poly-Si phase is dominating. The UST activation of the 0.9-eV band is also negligible in poly-Si films either deposited at 625 °C or in laser-recrystallized films with negligible amorphous fraction. Furthermore, the parameters of the 0.9-eV band are very close to a "defect" PL band previously observed in hydrogenated α-Si films [20]. Therefore, it is concluded that UST promotes a passivation of non-radiative centers both in the polycrystalline and amorphous phase of thin films.

4 UST mechanism

After plasma hydrogenation the total hydrogen concentration in poly-Si films can exceed the number of non-passivated dangling bonds by as much as two orders of magnitude [21]. Therefore, a significant reservoir of trapped electrically non-active hydrogen is available in poly-Si films after hydrogenation. In low-pressure CVD films obtained by decomposition of silane at 550 °C, the concentration of atomic hydrogen can be as much as 1 to 10 at. %. A substantial part of this hydrogen resides in the reservoir in a form of hydrogen molecules or hydrogen platelets [22]. It was suggested that UST enhances the hydrogenation of grain-boundary defects (such as dangling bonds) by a three-step mechanism schematically shown in Fig. 9: (a) UST hydrogen releasing from trapping states, (b) fast H-diffusion, and (c) hydrogen capture at dangling bonds [23]. It is obvious that UST releases of hydrogen from traps by a reduction of the hydrogen binding energy ΔE defined in (1). This picture has a remarkable similarity to the case of gas bubbles trapped on a glass wall and released after shaking them off (see the introduction).

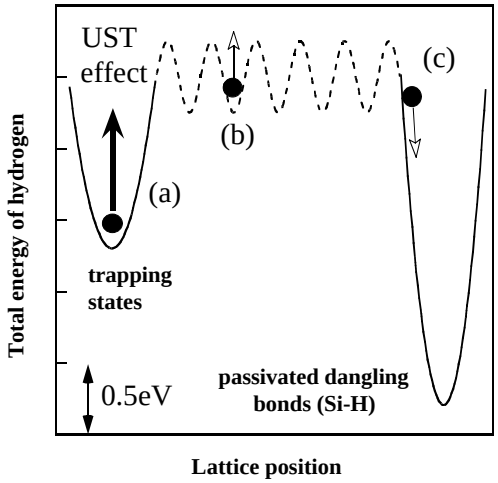

Fig. 9. The model of three-step UST enhanced hydrogenation in thin polycrystalline-Si is released from electrically non-active state into the bulk (a). The following fast hydrogen diffusion (b) and a capture at grain-boundary defects (c) accomplish UST processing

A physical reason for such UST-induced hydrogen detrapping is a selective absorption of the ultrasound by grain boundaries and other extended crystal defects where hydrogen can reside. Being liberated from traps, hydrogen can diffuse with the diffusion coefficient of the crystalline Si being $D_{\mathrm{Ho}} = 9.4 \times 10^{-3} \exp(-0.48\,\mathrm{eV}/kT)\mathrm{cm}^2/\mathrm{s}$. The UST activation energy of 0.33 eV is close to the 0.48 eV of H diffusion in crystalline silicon, however, the number is clearly smaller. A possible reduction of this energy can be attributed to UST-stimulated diffusion of hydrogen, according to the mechanism in [17]. The diffusion length L of H migration under UST ($T_{\mathrm{UST}} = 280\,^{\circ}\mathrm{C}$, $\Delta t = 3\,\mathrm{min}$) can be estimated as $L = (D_{\mathrm{H}}\Delta t)^{1/2} = 76\,\mu\mathrm{m}$. This value exceeds the 100-nm grain size of poly-Si films, which explains why liberated hydrogen can quickly approach non-radiative centers in poly-Si and α-Si phases.

The following consideration can account for the observed reduction of the hydrogen binding energy using ultrasound. It is known that the binding energy of hydrogen can be substantially perturbed in strained grain-boundary regions. As an example, in the strained Si–H–Si configuration, the binding energy of hydrogen linearly varies with stretching of Si–Si bond-length at the rate of 0.46 eV per 0.1 A [24]. This value is taken as a base line to estimate a UST effect on hydrogen binding. Under ultrasound, a dynamic stress field generates regions of local expansions and tensions. The amplitude of the average acoustic strain in our UST study is small, of the order of 10^{-3}, and corresponds to bond stretching of 2.5×10^{-3} Å. However, it is anticipated that the elastic modulus of grain boundaries is smaller than the modulus at inter-grain regions. In this case, UST stress will generate strong local strains at grain boundaries. To quantify the effect, we consider the ratio of grain-boundary volume to inter-grain volume as 1% for a 100-nm grain size. The amplitude of acoustic strain in the grain boundary will approach 10^{-1} corresponding to 10% stretching of bond-length by 0.25 Å, and a reduction of binding energy by ≈ 1 eV. This value is consistent with expected binding energy of the atomic hydrogen in the reservoir.

5 Application of UST

Ultrasound processing has an obvious interest as a means to improve the performance of electronic devices. We summarize in Table 2 several reported application results obtained in different research groups.

- UST processing was successfully applied to hydrogenated poly-Si thin-film transistors [25]. The reduction of leakage currents by a factor of 10, and a shift of threshold voltage by as much as 0.5 V at commercial TFTs, are consistent with the proposed model of UST-enhanced hydrogenation. These experiments demonstrate the utility of UST processing to upgrade hydrogenated poly-Si thin-film transistors in state-of-the-art active-matrix liquid-crystal displays.
- Hydrogenated amorphous carbon films are promising as blue electroluminescent diodes for flat-panel displays [31]. The experimental structures were designed at KAIST (Korea) and subjected to UST processing at temperatures up to 300 °C. A substantial and stable increase of EL efficiency by a factor of two was achieved.
- An improvement of ribbon silicon solar cell efficiency using UST was previously observed [27]. To assess the parameters of photovoltaic material, the minority carrier diffusion length was measured after various UST processing regimes in EFG crystalline Si-wafers. We have found a substantial UST increase by a factor of three of minority carrier diffusion length in the "bad" regions of wafers with originally low 10 to 15 μm diffusion length [32]. This UST effect may lead to a further upgrading of solar cell efficiency.

6 Summary

Ultrasound treatment applied to hydrogenated Si-based thin films is beneficial in improving their recombination and trans-

Table 2. Improvement of electronic devices using UST

Type of device	Material	Improved parameter	Upper limit of UST effect	Reference
Thin-film transistor	Poly-Si	Leakage current Threshold voltage	10 times lower 0.5 V lower	[25]
Tunnel diode	GaAs	Current noise	4 times lower	[26]
Solar cell	Crystalline poly-Si	Efficiency	5% higher	[27]
Light-emitting diode	InGaAs	Intensity	30% higher	[28]
	ZnS:Mn	Luminance	≈ 2 times higher	[29]
IR detector	CdHgTe	$1/f$ noise	10 times lower	[30]

port characteristics. The physical model consists in liberation of the trapped hydrogen by ultrasound from the electrically non-active state and passivation with this hydrogen of residual grain-boundary defects (dangling bonds). This process is applicable to poly-Si thin-film transistors and solar cells on glass substrates, where effective hydrogenation is a technological key process. Feasibility experiments in hydrogenated electronic devices justified the UST concept of defect engineering in semiconductors.

Acknowledgements. The author would like to thank N.E. Korsunskaya, M.K. Sheinkman, A.P. Zdebskii, J.H. Werner, S.V. Koveshnikov, J. Lagowski, L. Jstrzebski, F. Shimura, and B. Sopori for helpful discussions. The cooperation with A.U. Savchouk, and G. Nowak is greatly acknowledged.

References

1. I.V. Ostrovskii, V.N. Lisenko: Sov. Phys. Solid State **24**, 682 (1982)
2. S. Ostapenko, N.E. Korsunskaya, M.K. Sheinkman, S.V. Koveshnikov: In *Encyclopedia of Electrical and Electronics Engineering*, ed. by J.G. Webster (Wiley, New York 1999) in press
3. http://www.eng.usf.edu/ OSTAPENK/SMD
4. A.P. Zdebskii, S.S. Ostapenko, A.U. Savchuk, M.K. Sheinkman: Sov. Tech. Phys. Lett. **10**, 525 (1984)
5. L.V. Borkovskaya, B.R. Dzhumaev, I.A. Drozdova, N.E. Korsunskaya, I.V. Markevich, A.F. Singaevskii, M.K. Sheinkman: Physics of Solid State **37**, 1511, (1995)
6. S. Ostapenko, R. Bell: J. Appl. Phys. **77**, 5458 (1995)
7. S. Ostapenko, L. Jastrzebski, J. Lagowski, R.K. Smeltzer: Appl. Phys. Lett. **68**, 2873 (1996)
8. Y. Koshka, S. Ostapenko, T. Ruf, J. Zhang: Appl. Phys. Lett. **68**, 2537 (1996)
9. P.I. Baranskii, A.E. Belyaev, S.M. Komirenko, N.V. Shevcenko: Sov. Phys. Solid State **32**, 1257 (1990)
10. V.L. Gromashevskii, V.V. Dyakin, E.A. Sal'kov, S.M. Sklyarov, N.S. Khilimova: Ukr. Fiz. Zhurnal **29**, 550 (1984)
11. A. Makosa, T. Wosinski, Z. Witczak: Acta Phys. Pol. A **84**, 653 (1993)
12. V.P. Grabchak, A.V. Kulemin: Sov. Phys. Acoust. **22**, 475 (1976)
13. V.D. Krevchik, R.A. Muminov, A.Ya. Yafasov: Phys. Status Solidi A **63**, K159 (1981)
14. P. Zdebskii, N.V. Mironyuk, S.S. Ostapenko, A.U. Savchuk, M.K. Sheinkman: Sov. Phys. Semicond. **20**, 1167 (1986)
15. V.N. Babentsov, S.I. Gorban', I.Ya. Gorodetckii, N.E. Korsunskaya, I.M. Rarenko, M.K. Sheinkman: Sov. Phys. Semicond. **25**, 749 (1991)
16. G. Garyagdiev, I.Ya. Gorodetckii, B.R. Dzhumaev, N.E. Korsunskaya, I.M. Rarenko, M.K. Sheinkman: Sov. Phys. Semicond. **25**, 248 (1991)
17. V.N. Pavlovich: Phys. Status Solidi B **180**, 97 (1993)
18. A.U. Savchouk, S. Ostapenko, G. Nowak, J. Lagowski, L. Jastrzebski: Appl. Phys. Lett. **67**, 82 (1995)
19. H. Yokoyama, T. Inoue: Thin Solid Films **242**, 33 (1994)
20. R.A. Street: Advances in Physics **30**, 593 (1981)
21. N.H. Nickel, N.M. Johnson, W.B. Jackson: Appl. Phys. Lett. **62**, 3285 (1993)
22. N.H. Nickel, N.M. Johnson, C.G. Van de Walle: Phys. Rev. Lett. **73**, 3393 (1994)
23. S. Ostapenko: Materials Science Forum: **258-263**, 197 (1997)
24. C.G. Van de Walle, N.H. Nickel: Phys. Rev. B **51**, 2636 (1995)
25. S. Ostapenko, L. Jastrzebski, J. Lagowski, R.K. Smeltzer: Mater. Res. Soc. Symp. Proc. **424**, 201 (1997)
26. P. Zdebskii, M.I. Lisyanskii, N.B. Luk'yanchikova, M.K. Sheinkman: Sov. Tech. Phys. Lett. **13**, 421 (1987)
27. A. Iskanderov, V.D. Krevchik, R.A. Muminov, I.U. Shadybekov: Applied Solar Energy **24**, 21 (1988)
28. P. Zdebskii, V.L. Korchnaya, T.V. Torchinskaya, M.K. Sheinkman: Sov. Tech. Phys. Lett. **12**, 31 (1986)
29. V.G. Akul'shin, V.V. Dyakin, V.N. Lysenko, V.E. Rodionov: Sov. Phys. Tech. Phys. **34**, 1186 (1989)
30. Y.M. Olikh, Y.N. Shavlyuk: Phys. Solid State **38**, 1835 (1996)
31. J.-W. Lee, K.S. Lim: Appl. Phys. Lett. **68**, 1031 (1996)
32. S. Ostapenko, L. Jastrzebski, J. Lagowski, B. Sopori: Appl. Phys. Lett. **65**, 1555 (1994)